EVALUATION OF NEARSHORE WAVE MODELS IN STEEP REEF ENVIRONMENTS

Mark Buckley[1] and Ryan Lowe[1]

Abstract

To provide coastal engineers and scientists with a quantitative evaluation of nearshore numerical wave models in reef environments, we review and compare with laboratory observations three commonly used models. These models are: SWAN (Booij et al., 1999), a phase-averaged spectral wave model, SWASH (Zijlema et al., 2011) a phase-resolving nonlinear shallow water wave model with added non-hydrostatic terms, and XBeach (Roelvink et al., 2009) a coupled phase-averaged spectral wave model for sea-swell and nonlinear shallow water model for infragravity waves. Models were assessed for their performance in predicting bulk sea-swell (SS) wave height, infragravity (IG) wave height, wave spectra, and wave setup ($\bar{\eta}$) at 9 locations across the fringing reef profile of Demirbilek et al. (2007). Simulations were performed with the "recommended" coefficients as documented for each model, and then key breaking parameters (γ in both SWAN and XBeach, and α in SWASH) were optimized in a sensitivity analysis. SWAN, SWASH, and XBeach were found to be capable of predicting SS wave height variations across the steep fringing reef profile with reasonable accuracy. Nevertheless, with tuning of the key breaking parameters the accuracy of predictions was further increased significantly. SWASH and XBeach were also able to predict bulk IG wave height and spectral transformation. Although SWAN was capable of modeling bulk SS wave height, in its current form it was not capable of modeling the observed spectral transformation, as evident in the under prediction of IG wave height.

Key words: Wave breaking, bottom friction, nonlinear waves, steep slope, coral reefs, numerical modeling

1. Introduction

To provide coastal engineers and scientists with a quantitative evaluation of nearshore numerical wave models in reef environments, we review and compare with laboratory observations three commonly used models. Nearly all nearshore wave models have primarily (or exclusively) been developed, calibrated, and tested on sandy beaches having mild slopes. As a result it is unclear if these models are suitable to simulate waves in reef systems, given that reefs have much more complex morphologies and extreme slopes (in some cases approaching near vertical). Here we review three commonly used nearshore wave models and quantitatively compare model results with data from a comprehensive laboratory experiment. These models are: SWAN (Booij et al., 1999), a phase-averaged spectral wave model, SWASH (Zijlema et al., 2011) a phase-resolving nonlinear shallow water wave model with added non-hydrostatic terms, and XBeach (Roelvink et al., 2009) a coupled phase-averaged spectral wave model for sea-swell and nonlinear shallow water model for infragravity waves. This review and comparison provides insight into the suitability of each model to simulate a full range of hydrodynamic processes (sea-swell, infragravity waves and wave setup) within reef systems, and an assessment of where each model tends to break down and thus be improved.

Numerical wave models used to investigate field scale (of order kilometres to 100s of kilometres) processes loosely fall into two categories: stochastic (phase-averaged) and deterministic (phase-resolving) (Sheremet et al., 2011). Stochastic models simulate wave processes in a probabilistic manner, often based on empirical formulations calibrated to field or laboratory data. Deterministic models often simulate wave processes based on the conservation laws (mass and momentum), and may also include empirical formulations calibrated to field or laboratory data. Deterministic models resolve individual waveforms, requiring a grid resolution fine enough to capture the shortest wave length (highest frequency) waves of interest in a study. Adding to the computational demand, the maximum allowable computational time step required to resolution wave propagation is proportional to the grid resolution. Due to the computational demand, the application of phase resolving models is restricted to studies of lower frequency motions (e.g. long-waves and currents), or small scale (e.g. a harbor entrance) and short duration, or idealised one-dimensional studies. Stochastic models, on the other hand, do not have the same restriction on grid

[1]School of Earth and Environment, University of Western Australia, 35 Stirling Highway, Crawley WA 6009, Australia. 21003158@student.uwa.edu.au

resolution or time steps allowing much larger scale and longer term studies to be conducted. For larger scale (longer duration) studies which require modelling physical processes at a range of frequencies (e.g. wind-waves, tides, and currents) deterministic and stochastic models are often coupled.

The underlying assumptions embedded in nearshore models originally developed in mild slope beach environments are often technically violated when applied to reef environments (Massel and Gourlay (2000), Sheremet et al. (2011), Demirbilek and Nwogu (2007)). For example, steep slopes may violate the mild slope assumption found in many models (Demirbilek and Nwogu, 2007). Additionally, parameterizations of bed stress, breaking, and other processes developed in beach environments and found in many models may not be applicable. Due to rapid bathymetric change on reef slopes wave breaking is particularly intense and occurs over a much smaller area then the broad surf zone found on dissipative beaches. In the field study of Lowe et al. (2005) the importance of bottom friction over the irregular bathymetry is highlighted. Shoreward of the break point infragravity waves constitute a significant portion of the total wave energy (e.g. Hardy and Young (1996), Péquignet et al. (2009), and Pomeroy et al. (2012)) and resonance may occur (Péquignet et al., 2009).

Despite these theoretical limitations, models and parameterizations originally derived for mild sandy slopes have been applied to steep slope reef environments with little or no modification. Symonds et al. (1995) first formulated a one-dimensional (1D) analytical model for wave driven currents on reefs, based on a linearized set of momentum equations and radiation stress theory. Subsequent 1D analytical models have been formulated by Hearn (1999) and Gourlay and Colleter (2005). Sheremet et al. (2011) compared several 1D nonlinear stochastic and deterministic numerical models to laboratory data. Demirbilek and Nwogu (2007) and others have applied 1D Boussinesq-type models. Buckley et al. (2011) applied a Boussinesq-type model to simulate overtopping of a fringing reef / dune system during a hurricane. Phase-averaged spectral wave models have been applied in field studies by Lowe et al. (2009), Hoeke et al. (2011), and Storlazzi et al. (2011), and tested against laboratory and field data by Filipot and Cheung (2012). Zijlema (2012) and Torres-Freyermuth et al. (2012) applied a non-hydrostatic nonlinear shallow water wave model to laboratory and field datasets. Pomeroy et al. (2012) and Van Dongeren et al. (2013) applied a coupled wave action and nonlinear shallow water model to field data.

In this present study, three nearshore wave models are reviewed, applied to a laboratory data set, and quantitatively compared. In Section 2, the models are reviewed with key depth-limited breaking and frictional dissipation terms highlighted. Each model was then applied to 29 comprehesive laboratory test conditions of Demirbilek et al. (2007). Simulations were performed with the "recommended" coefficients as documented for each model. This provideds a estimate of the errors expected in the application of an untuned model. Of the 29 test conditions six representative conditions were selected for further sensitivity analysis of the key depth-limited breaking parameter for each model. Sensitivity analysis gives insight into the improvement that can be gained from tuning the key breaking parameters and an indication of the range in the optimum values for key breaking parameters that can be expected for each model. Models were assessed for their performance in predicting bulk sea-swell (SS) wave height, infragravity (IG) wave height, wave spectra, and wave setup ($\bar{\eta}$) at 9 locations across the fringing reef profile.

2. Numerical models

In this study, three common nearshore wave models (Table 1) were used. These models were selected as they are all open-source, widely used, and also span a range of numerical approaches (both spectral and phase-resolving), theoretical complexities, and computational demands. SWAN (Simulating Wave Nearshore; Version 40.91 downloaded from http://swanmodel.sourceforge.net) (Booij et al., 1999) is a stochastic (phase-averaged) spectral wave model. SWASH (Simulating WAves till Shore; Version 1.20 downloaded from http://swash.sourceforge.net) (Zijlema et al., 2011) is a deterministic non-hydrostatic free-surface model. XBeach (Version 19; downloaded from http://oss.deltares.nl/web/xbeach) (Roelvink et al., 2009) is a nearshore wave and circulation model that combines stochastic and deterministic approaches. As detailed descriptions of these three models are available widely in the literature, only a brief overview is included here.

Model	**Class**	**Breaking formulation**	**Reference**
SWAN	Wave action balance	Parametric	(Booij et al., 1999)
XBeach	Wave action balance with phase resolving IG	Parametric	(Roelvink et al., 2009)
SWASH	NLSW+ non-hydrostatic terms	Shock-capturing	(Zijlema et al., 2011)

Table 1: Open source numerical models evaluated in this study.

SWAN predicts the spectral evolution of wave action in space and time (Booij et al., 1999). Wave action is defined as $A=E/\sigma$, where $E(\sigma, \theta)$ is wave variance spectrum that distributes wave energy over frequencies (σ) and propagation directions (θ). The wave action equation is stated as (Booij et al., 1999),

$$\frac{\partial A}{\partial t}+\frac{\partial c_x A}{\partial x}+\frac{\partial c_y A}{\partial y}+\frac{\partial c_\sigma A}{\partial \sigma}+\frac{\partial c_\theta A}{\partial \theta}=-\frac{S_{tot}}{\sigma} \quad (1)$$

where, c_x, c_y, c_σ, and c_θ are the propagation velocities of wave energy in spatial (x, y), spectral (σ), and directional (θ) space respectively. S_{tot} can include dissipation terms, in particular due to depth-limited breaking and bottom friction, as well as growth terms.

SWASH solves the nonlinear shallow water equations with added non-hydrostatic pressure (Zijlema et al., 2011). Smit et al. (2013) describes the governing equations in Cartesian coordinates (x, z), and time (t), as,

$$\frac{\partial u}{\partial t}+\frac{\partial uu}{\partial x}+\frac{\partial wu}{\partial z}=-\frac{1}{\rho}+\frac{\partial (p_n+p_{nh})}{\partial x}+\frac{\partial \tau_{xz}}{\partial z}+\frac{\partial \tau_{xx}}{\partial x} \quad (3)$$

$$\frac{\partial w}{\partial t}+\frac{\partial uw}{\partial x}+\frac{\partial ww}{\partial z}=-\frac{1}{\rho}\frac{\partial p_{nh}}{\partial z}+\frac{\partial \tau_{zz}}{\partial z}+\frac{\partial \tau_{zx}}{\partial x} \quad (4)$$

$$\frac{\partial u}{\partial x}+\frac{\partial w}{\partial z}=0 \quad (5)$$

where $u(x,z,t)$ and $w(x,z,t)$ are the horizontal and vertical velocities respectively; p_h and p_{nh} are the hydrostatic and non-hydrostatic pressures, and τ_{xx}, τ_{xz}, and τ_{xz} are the turbulent stresses.

XBeach models short-wave processes in a stochastic manner, solving the phase-averaged wave action equation (Roelvink et al., 2009). The wave action equation implemented in XBeach is very similar to that of SWAN with the difference being that in XBeach the wave action equation is only solved for a single representation frequency. However, in XBeach the infragravity wave motions and mean flows are modelled in a deterministic manner, solving the nonlinear shallow water equations using a finite difference scheme (Roelvink et al. 2009).

2.1. *Wave breaking*

There is no analytical solution for wave breaking and commonly used depth-integrated numerical wave models do not describe overturning of the free-surface and thus cannot fully reproduce wave breaking processes (Cienfuegos et al., 2010). Stochastic models commonly use empirical (parametric) formulations to predict the rate of wave energy dissipation during the wave breaking process. These formulations generally include a method for estimating the probability distribution of broken waves and apply an energy dissipation rate using a theory for idealized bores (Apotsos et al., 2007). SWAN and XBeach both implement parametric breaking formulations

SWAN (by default) uses the Battjes and Janssen (1978) formulation (here after BJ78). BJ78 calculates the mean energy dissipation due to depth-limited breaking, D_b, as

$$D_b=\frac{1}{4}\rho g f_{mean} B Q_b H_{max}^2 \quad (6)$$

where ρ is density, g is gravity, f_{mean} is mean frequency, B is the breaking intensity coefficient (by default $B=1$), and Q_b is the fraction of broken waves. The value of D_b depends critically on the "breaker parameter" $\gamma=H_{max}/h$ (in which H_{max} is the maximum possible individual wave height in the local water depth h). Untuned γ=0.73 for BJ78. Q_b is estimated using a Rayleigh wave height distribution truncated at H_{max}.

$$\frac{1-Q_b}{\ln Q_b} = -8\frac{E_{tot}}{H_{max}^2} \quad (7)$$

where E_{tot} is the total wave energy variance.

XBeach (by default) uses a modified form of the parametric dissipation formulation of Roelvink (1993) (here after R93). Wave dissipation due to depth-limited breaking, is calculated as

$$D_b = 2f_p B Q_b E_{tot}\frac{H_{rms}}{h} \quad (9)$$

where f_p is the peak frequency and B is the breaking intensity coefficient (by default B=1). The fraction of broken/ breaking waves is calculated as (Roelvink, 1993)

$$Q_b = 1 - exp\left[-\left(\frac{H_{rms,}}{H_{max}}\right)^{10}\right], H_{rms} = \sqrt{\frac{8E_{tot}}{\rho g}}, H_{max} = \frac{\gamma \tanh kh}{k} \quad (10)$$

where k is wave number. Untuned γ=0.55 for R93.

Deterministic models of the Boussinesq-type commonly include breaking effects by adding an ad-hoc dissipation term to the momentum equations (e.g. Svendsen (1984), Schäffer et al. (1993), and Madsen et al. (1997)). This method is referred to as an eddy viscosity approach. Eddy viscosity formulations require scaling coefficients with no direct physical or measurable meaning (Cienfuegos et al., 2010). The nonlinear shallow water equations can be formulated to satisfy exact conservation laws (flow volume and momentum) for non-dispersive waves (Zijlema and Stelling, 2008). Implementation of the exact conservation laws and use of numerical shock-capturing schemes, which solve discontinuous problems, allow breaking wave dissipation to be modeled in a manner similar to hydraulic jumps (Zijlema and Stelling, 2008).

SWASH accounts for depth-limited breaking with a shock-capturing conservation scheme (Zijlema and Stelling, 2008). In SWASH, with a large number of vertical layers, as waves steepen and approach breaking, a saw tooth waveform develops. At the discontinuity, energy is dissipated numerically via the shock-capturing scheme (Zijlema et al., 2012). With a single vertical layer, the saw tooth waveform is unable to develop due to the lack of vertical resolution of flow velocity. This requires an additional metric to determine the onset of breaking (Zijlema et al., 2012). When

$$\frac{\partial \eta}{\partial t} > \alpha\sqrt{gh} \quad (11)$$

where η is free surface elevation, the non-hydrostatic pressure terms are neglected and remain so at the front face of the breaker, allowing for a saw tooth waveform (Smit et al., 2013). The parameter $\alpha > 0$ determines the onset of the breaking process. The untuned value of α=0.60 is advised, which corresponds to a local front slope of ~30^o.

2.2. *Bottom stress*

Wave energy and flow momentum are dissipated due to bottom stresses, related to the turbulent vertical fluxes of horizontal momentum (Feddersen et al., 2003). Wave and current bottom stresses are commonly treated independently using quadratic bottom friction formulations with an empirical friction coefficient. SWAN and XBeach both add a term for wave energy dissipation due to bottom roughness to the wave action equation. SWASH and XBeach both add terms to the momentum equations to account for dissipation due to bottom roughness.

3. Application

Laboratory experiments by Demirbilek et al. (2007) were used to assess the performance of each of the numerical models. Their study consisted of 80 tests conditions (of which 29 have negligible wind forcing and are used here) carried out on a 1 in 64 scale model of a fringing reef type profile typical of the southeast coast of Guam, conducted in a wind-wave flume at the University of Michigan (UM). Figure 1 shows the experimental setup. The flume was 35 m long, 0.7 m wide and 1.6 m high, with smooth walls and a smooth plastic bed. The fringing reef profile consisted of a composite slope with a 1 in 10.6 fore reef slope, a horizontal reef flat, and a 1 in 12 sloping beach. Water surface elevations were measured by 9 capacitance type wave gauges and runup was measured by a

capacitance type wave gauge oriented along the beach slope. Irregular waves with significant wave heights up to 10 cm with peak periods from 1.0 to 2.5 s were generated with a wedge type wave maker. A JONSWAP spectrum with peak enhancement factor 3.3 was used. Laboratory tests were conducted in the flume with different combinations of bulk sea-swell rms wave height ($H_{rms,SS}$), peak period (T_p), and still water depth over the reef flat (h_r).

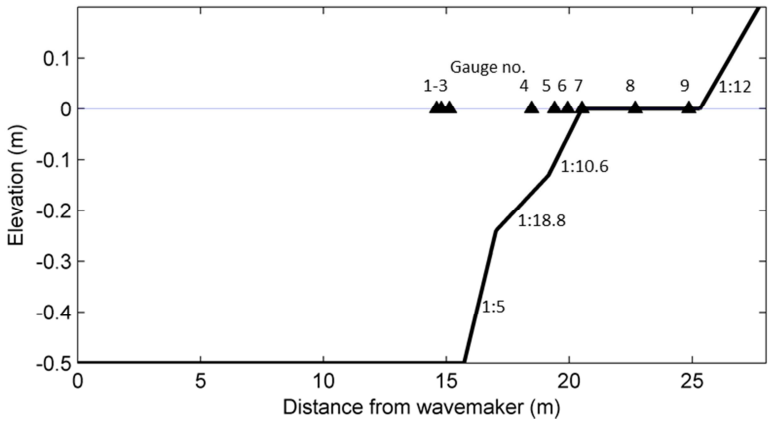

Figure 1: Laboratory setup for the University of Michigan flume experiment (Demirbilek et al., 2007).

3.1. *Model setup*

Numerical simulations were performed with each model configured in a one-dimensional mode using a grid size of 0.02 m with a minimum threshold water depth of 0.005 m. SWASH and XBeach simulations were run for periods of 900 s, with a time step determined by imposing a maximum Courant number of 0.5. SWAN simulations were performed in a stationary mode. All models were forced on the offshore boundary with a wave energy spectra derived for each test condition from the measured water level time series at the offshore gauges. Directional (i.e., shoreward versus seaward) filtering of the offshore water level gauges was performed to remove reflected wave energy using the three point method of Mansard and Funke (1980). To simulate the smooth plastic bed of the UM flume a dimensionless friction coefficient of c_f=0.001 was used. The low c_f value was included for model stability, but has a negligible contribution to the overall wave dissipation (overwhelmingly dominated by wave breaking). The wave action equations for SWAN and XBeach include an optional term of wave friction, by default this term is neglected in XBeach and included in SWAN. Here we do not include wave friction in the simulations. This is in line with Filipot and Cheung (2012), who neglect wave friction when applying SWAN to the UM dataset.

Following Zijlema et al. (2012), SWASH was run with the discrete upwind momentum advection scheme. Depth-limited wave breaking was accounted for with the onset of breaking controlled by α=0.60 in the untuned case. α was varied from 0.1 to 3.0 in increments of 0.1 in the sensitivity analysis. Water level time series output from the model were exported at the gauge locations at 20 Hz.

SWAN was run in stationary mode with triad interactions and frequency shifts activated, wave setup activated, and white capping deactivated. The simulations were performed with 36 directional bins from 0 to 360^o, and 42 frequency bins from 0.01 to 10 Hz. Depth-limited wave breaking was modeled using the BJ78 formulation with γ=0.73 and B=1 for the untuned case. γ was varied from 0.1 to 1.2 in increments of 0.05 in the sensitivity analysis. Wave energy spectra were exported at the gauge locations.

Depth-limited wave breaking in XBeach was modeled using the R93 formulation with γ=0.55 and B=1 for the untuned case. Like SWAN, γ was varied 0.1 to 1.2 in increments of 0.05 in the sensitivity analysis. By default XBeach includes a roller energy balance; this was left activated in the current study with the default *beta* (roller face slope (Reniers, 1997)) value of 0.1. Water level time series where exported at the gauge locations at 20 Hz.

3.2. *Data processing and performance metrics*

Measured and simulated water level time series were used to compute one-dimensional wave energy spectra *S(f)* using the Welch's averaged, modified periodogram method with a Hanning window and a chunk size of 2^{10} samples

(~50 seconds). The bulk sea-swell (SS) rms wave height, $H_{rms,SS}$ was calculated as

$$H_{rms,ss} = \sqrt{8\int_{f_l}^{\infty} S\,df} \tag{12}$$

where f_l is the boundary between SS and infragravity (IG) frequency bands. In agreement with Sheremet et al. (2011) and others f_l was taken as half the peak forcing frequency of each simulation (i.e. f_l=0.5f_p). XBeach uses a representative frequency for the SS band and does not model the SS spectra, thus the mean $H_{rms,SS}$ for XBeach was exported directly from the model.

Likewise, bulk IG rms wave height, $H_{rms,IG}$ was calculated as

$$H_{rms,IG} = \sqrt{8\int_{0}^{f_l} S\,df} \tag{13}$$

Following, Apotsos et al. (2008) model performance was quantified using the weighted rms percent error metric (*WRPE*), defined as

$$WRPE = \sqrt{\sum_{n}\left[\left(\frac{obs_n - pred_n}{obs_n}\right)^2 * weight_n\right]} * 100\% \tag{14}$$

$$weight_n = \frac{dist_{n-1} + dist_{n+1}}{dist_{tot}} \tag{15}$$

where *n* is the gauge number, *obs* and *pred* are the observed and predicted values, and *dist* is the distance between gauges. *WRPE* was calculated for $H_{rms,ss}$ and $H_{rms,IG}$ (here after *WRPE SS* and *WRPE IG* respectively). Offshore gauges used for the forcing condition were excluded and only Gauges 5-9 (Figure 1) were used in the calculation. Model tuning was assessed using *WRPE SS*. *WRPE SS* is used rather than a combination of *WRPE SS and WRPE IG* as depth-limited wave breaking occurs primarily in the SS frequency band. The percent error reduction that can be achieved with model tuning was also estimated from the Brier Skill Score (*BSS*) (Apotsos et al., 2008).

$$BSS = \left[1 - \frac{WRPE_{tuned}}{WRPE_{untuned}}\right] * 100\% \tag{16}$$

BSS was calculated for *WRPE SS* and *WRPE IG* (here after *BSS SS* and *BSS IG* respectively).

4. Results and Discussion

Laboratory observations showed rapid dissipation of SS energy at the reef crest, an increase in the proportion of IG energy over the reef flat, and wave setup across the reef. Figure 2 gives an example of SS and IG transformation across the fringing reef profile for Test no. 35 ($H_{rms,ss}$=0.032 m; T_p=1.42; h_r=0.00 m). Breaking occurs at the reef crest with the largest dissipation of SS and IG energy between Gauges 6 and 7 (Figure 2). With untuned breaking parameters, SWASH (α=0.60) and SWAN (γ=0.73 and B=1) match this dissipation and the overall bulk SS transformation well. XBeach (γ=0.55 and B=1) only slightly underestimates the dissipation at the break point, somewhat over predicting $H_{rms,SS}$ on the reef flat. Tuning γ for XBeach gives a smaller than untuned optimum γ value of 0.35 (untuned γ=0.55), correcting the over prediction of $H_{rms,ss}$ and reducing the *WRPE SS* by 82% (Figure 2; Table 2). Tuning SWAN gives a greater than untuned optimum γ value of 0.85 (untuned γ=0.73) with a *WRPE SS* reduction of 73% (Table 2). Tuning SWASH gives a greater than untuned optimum α value of 2.9 (untuned α=0.60) with a *WRPE SS* reduction of 81% (Table 2).

				SWASH			SWAN			Xbeach		
Test no.	$H_{rms,SS}$	*Tp*	*hr*	Tuned α	*BSS SS* (%)	*BSS IG* (%)	Tuned γ	*BSS SS* (%)	*BSS IG* (%)	Tuned γ	*BSS SS* (%)	*BSS IG* (%)
19	0.059	2.56	0.051	1.4	39	-20	0.70	55	-2	0.30	73	-156
20	0.043	1.25	0.051	0.90	71	-1	0.80	84	0	0.35	89	48
21	0.058	1.83	0.051	1.2	75	6	0.73	0	0	0.35	84	23
33	0.041	1.02	0	1.3	14	18	0.90	67	1	0.35	81	-21
35	0.032	1.42	0	2.9	81	19	0.85	73	0	0.35	82	57
39	0.056	2.56	0	1.3	22	2	0.80	19	0	0.40	74	-3

Table 2: Results for optimization of the breaking tuning parameter γ in both SWAN and XBeach and α in SWASH. Tuned values of the coefficients and percent error reduction owing to model tuning (*BSS*) are given for six test cases

For Test no. 35 ($H_{rms,ss}$=0.032 m; T_p=1.42; h_r=0.00 m) model performance for IG transformation was more varied (Figure 2). SWASH and XBeach reproduced the overall IG development. However, XBeach over predicted $H_{rms,IG}$ and SWASH under predicted $H_{rms,IG}$ on the reef flat. Tuning the key breaking parameters for SWASH (α) and XBeach (γ), to minimize *WRPE SS*, also improved the prediction of $H_{rms,IG}$ (Figure 2). SWAN greatly under predicted IG energy across the reef profile, and showed nearly complete dissipation of IG energy on the reef flat. Trends in $\bar{\eta}$ over the reef profile for Test no. 35 were well-predicted with SWASH and XBeach, but under predicted using SWAN (Figure 2). $\bar{\eta}$ predictions were improved by tuning the key breaking parameters (Figure 2).

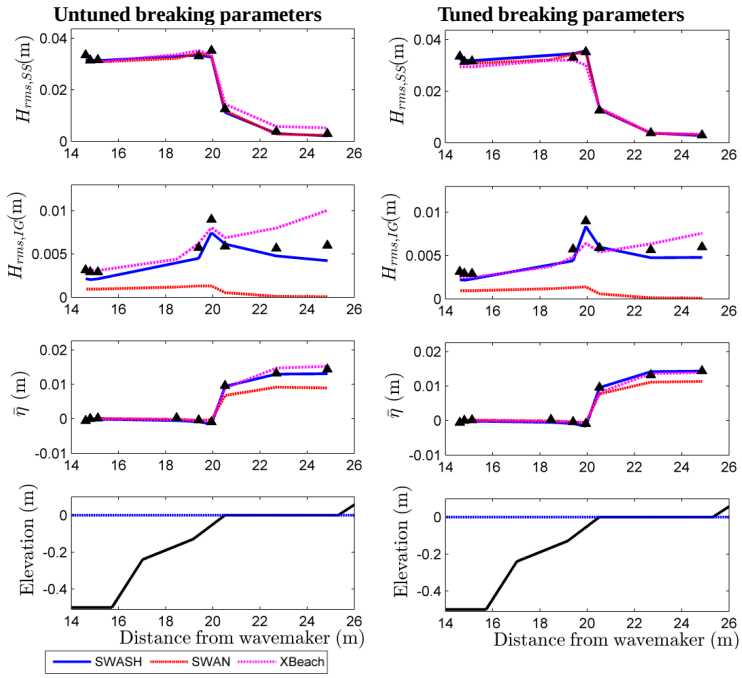

Figure 2. Measured (black triangles), and simulated $H_{rms,SS}$, $H_{rms\ IG}$ and $\bar{\eta}$ across the UM fringing reef profile for Test no. 35 ($H_{rms,SS}$=0.032 m; T_p=1.42; h_r=0.00 m). Model results for untuned (left column) and tuned (right column) breaking parameters are shown for SWASH (solid blue curve), SWAN (dotted red curve), and XBeach (dashed magenta curve). The reef elevation profile is shown in the bottom row for reference.

Measured and predicted wave spectra are shown for Test no. 35 in the shoaling region (Gauge 6; Figure 3) and on the reef flat (Gauge 8; Figure 3). At Gauge 6 the majority of the energy was in the SS band at the peak forcing frequency (given by the vertical black line; Figure 3). Measured energy in the IG band was relatively constant between these two gauges. Directional (i.e., shoreward versus seaward) analysis of the offshore water level showed a significant proportion of IG energy was directed offshore. SWASH and SWAN accurately predicted the distribution

of SS energy in the shoaling region (Gauge 6; Figure 3) and the dissipation of SS energy on the reef flat (Gauge 8; Figure 3). XBeach simulates SS using a representative frequency, so it is only possible to show the low-frequency spectra for XBeach.

SWASH (α=0.60) and XBEACH (γ=0.55 and B=1) with untuned breaking parameters showed a reasonable agreement with the measured wave heights (both $H_{rms,SS}$ and $H_{rms,IG}$) and $\bar{\eta}$ for the 29 test conditions (Figure 4). SWAN (γ=0.73 and B=1) accurately predicted $H_{rms,SS}$ and $\bar{\eta}$, but failed to capture the $H_{rms,IG}$. For all three models, the accuracy of $H_{rms,SS}$ and $\bar{\eta}$ predictions were improved by tuning the wave breaking parameters (Table 2; Figure 5). However, tuning the key breaking parameters to minimize *WRPE SS*, showed mixed results from the accuracy of the $H_{rms,IG}$ prediction, with some tests showing an improvement, while others showed decreased accuracy in the $H_{rms,IG}$ predictions (Table 2).

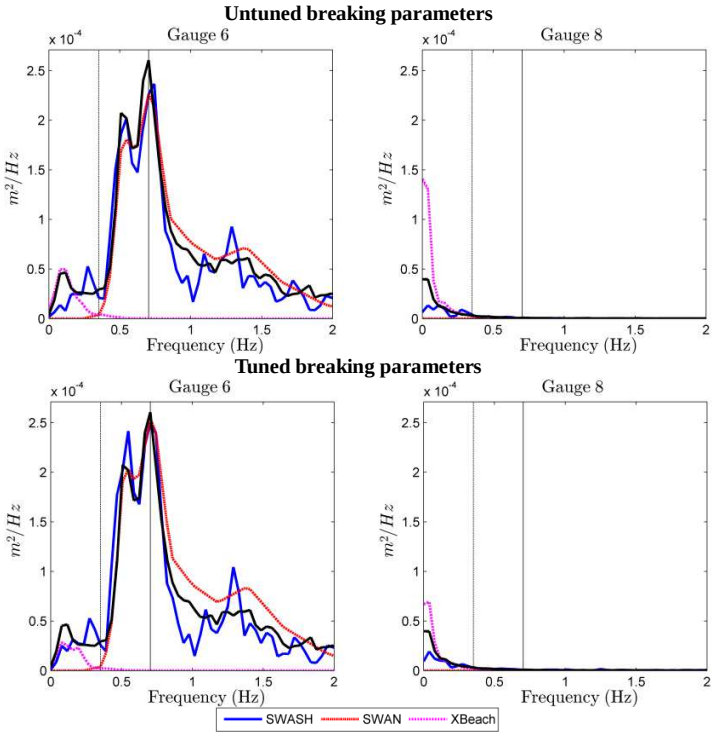

Figure 3. Measured (black solid curve) and simulated wave energy spectra at Gauge 6 (shoaling region; left column) and Gauge 8 (reef flat; right column) for Test no. 35 ($H_{rms,SS}$=0.032 m; T_p=1.42; h_r=0.00 m). Model results for untuned (upper row) and tuned (lower low) breaking parameters are shown for SWASH (solid blue line), SWAN (dotted red line), and XBeach (dashed magenta line). The peak forcing frequency (vertical solid black line) and SS-IG cut-off (vertical dashed black line) are shown for reference. XBeach simulates SS using a representative frequency, so it is only possible to show the low-frequency spectra for XBeach.

For the six test conditions chosen for sensitivity analysis, XBeach with the R93 breaking formulation showed consistently higher optimum γ values than the untuned value (Table 2). The average optimum γ for these test conditions was 0.35 (untuned γ=0.55). However, in contrast to XBeach, higher tuned values of γ~0.80 (untuned γ=0.73) were found for SWAN using BJ78. Though, γ is defined similarly in both R93 and BJ78, in practise γ is used as a model tuning parameter, and it is not unexpected that both the untuned and tuned values of γ differ between the two models. However, it is interesting that smaller than untuned optimum γ values are found for XBeach with R93, whereas larger than untuned optimum γ values are found for SWAN with BJ78. This may reflect slight differences in the response of these two breaking formulations on steep reef slopes.

Filipot and Cheung (2012) using the same UM dataset and SWAN with the BJ78 breaking formulation found an optimum γ value of 0.94 with a breaking intensity coefficient, B of 1.04. Similar to results presented here, the tuned γ value is greater than the untuned value of 0.73. The difference in the tuned values were likely due to the different

values of B (this was also optimized by Filipot and Cheung (2012), while we held this constant at B=1 here) and more importantly that Filipot and Cheung (2012) tuned γ to the total bulk wave height, thus including IG wave motions, whereas we tuned γ to just the SS wave height. This discrepancy in methods highlights the need for consistency when comparing coefficient values.

The increased tuned γ values, for SWAN with BJ78, found by Filipot and Cheung (2012) and in the present investigation are consistent with the trend in bottom slope empirically predicted by Nelson (1987) for mild slopes. Nelson (1987) found the dependence, of γ on bed slope (β) to be

$$\gamma = 0.55 + 0.88\exp[-0.012\cot(\beta)] \tag{17}$$

The Nelson (1987) formula predicts that γ would vary from 0.55 for horizontal slopes to 1.33 for the 1:10.6 slope in the UM fringing reef profile.

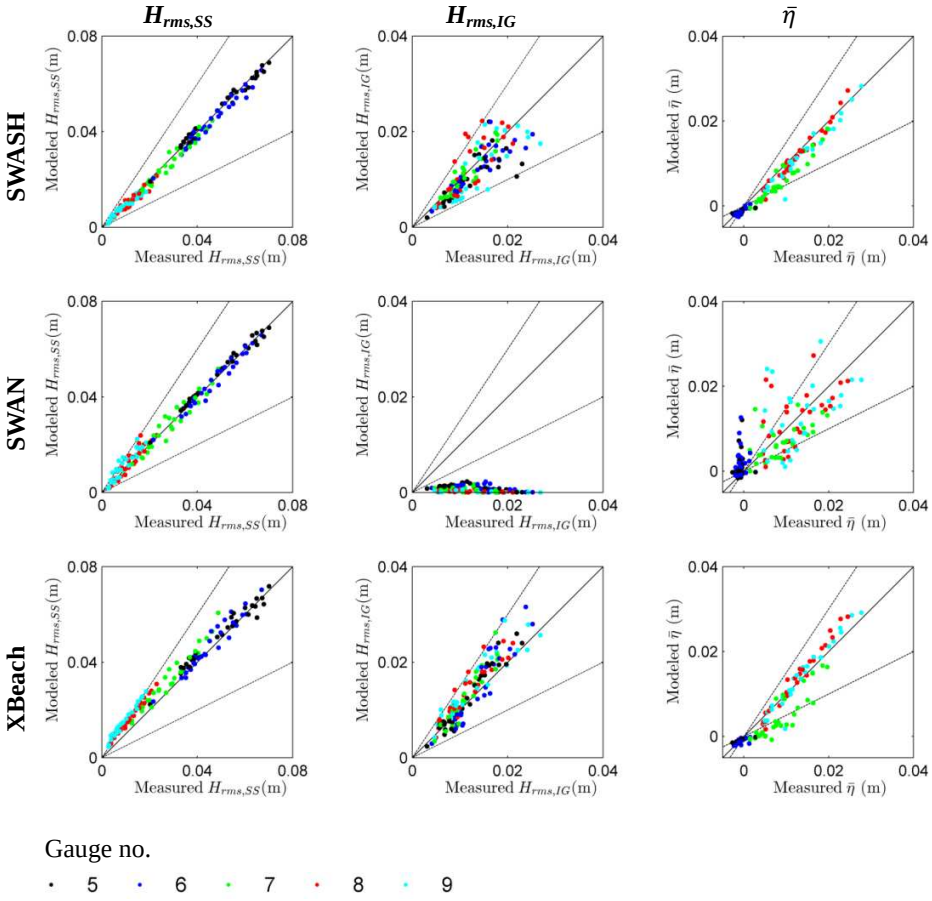

Figure 4. Comparison between measured and modeled $H_{rms,SS}$ (first column), $H_{rms,IG}$ (second column), and $\bar{\eta}$ (third column) for all test conditions. Measured values are given on the x-axis and simulation results are given on the y-axis for SWASH (first row), SWAN (second row), and XBeach (third row) with untuned breaking parameters. The 1:1 line (solid black diagonal lines) and 50% error bounds (dashed black lines) are given for reference. Point colors correspond to gauge locations (given below the plots).

Tuned γ values for R93 in XBeach were consistently smaller than the untuned value of 0.55. This is in contrast to the findings for SWAN with BJ78 (both in the present study and in Filipot and Cheung (2012)) and the slope dependence predicted by Nelson (1987).

The α breaking parameter for the shock-capturing scheme in SWASH controls the onset of breaking by neglecting non-hydrostatic terms when $\partial\eta/\partial t > \alpha\sqrt{gh}$. Increasing α, increases the threshold surface slope for the on-set of

breaking, thus delaying breaking. For the six test conditions chosen for sensitivity analysis, optimum tuned α values were considerably higher than the untuned value of 0.60, with an average value of 1.5. α=1.5 corresponds to a steeper sloping wave face (~55^o) than the untuned α=0.60 (~25^o), which would be physically consistent with the occurrence of plunging breakers on the steep fore reef slope. As depicted in Figure 4, SWASH results with the untuned α=0.60 agree well with measurements, but improvement is possible by tuning α (Table 2; Figure 5).

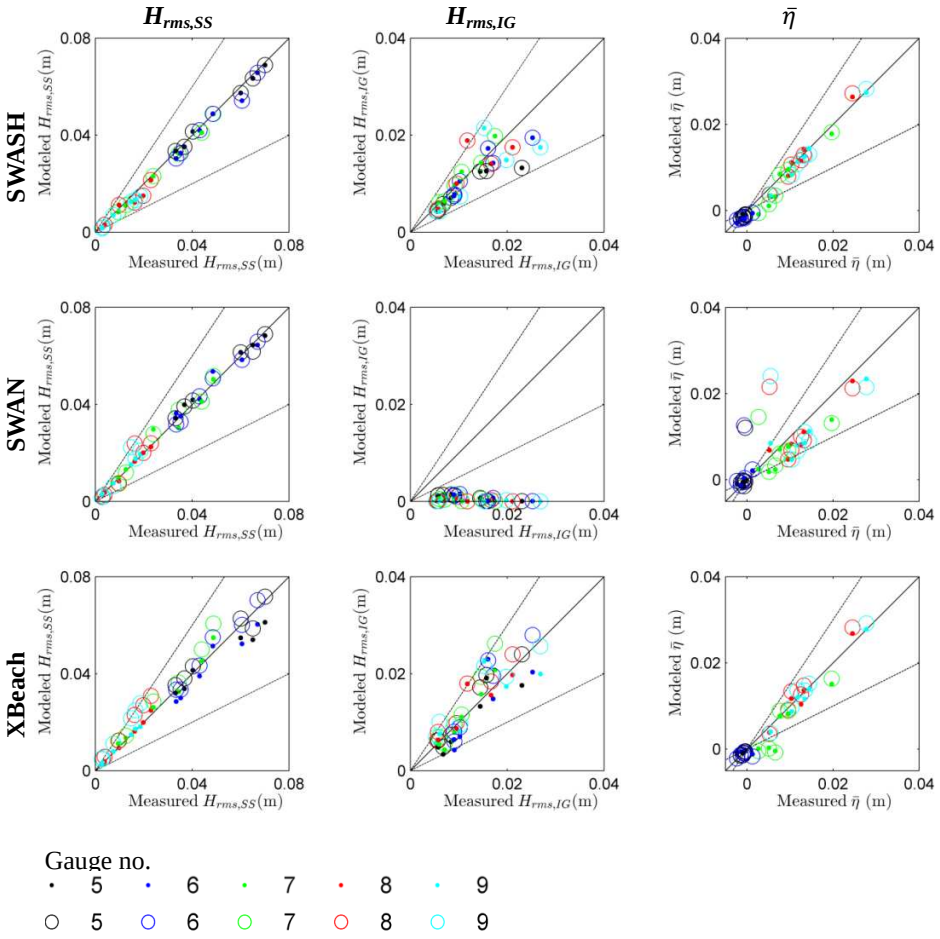

Figure 5. Comparison between measured and modeled $H_{rms\ SS}$ (first column), $H_{rms,IG}$ (second column), and $\bar{\eta}$ (third column) for test conditions were breaking parameters are tuned (Table 2). Measured values are given on the x-axis and simulation results are given on the y-axis for SWASH (first row), SWAN (second row), and Xbeach (third row) with untuned breaking parameters (open circles) and tuned parameters (solid dots). The 1:1 line (solid black diagonal lines) and 50% error bounds (dashed black lines) are given for reference. Point colors correspond to gauge locations (given below the plots).

5. Conclusions

In this test of three commonly used wave models (SWAN, SWASH, and XBeach), all were found to be capable of predicting bulk SS wave height variations across the steep fringing reef profile with reasonable accuracy (Figure 4 column 1). Nevertheless, with tuning of the breaking parameters (γ in both SWAN and XBeach, and α in SWASH) the accuracy of predictions can be further increased significantly (Table 2; Figure 5 column 1). SWASH and XBeach were also able to predict bulk IG wave height (Figure 4 column 2; Figure 5 column 2) and spectral transformation (Figure 3), albeit with higher error. Although SWAN is capable of modeling bulk SS, in its current form it is not capable of modeling the observed spectral transformation, as evident in the under prediction of IG waves across the reef flat (Figures 2, 3, 4, and 5). Sheremet et al. (2011) show that it is possible to accurately model spectral

transformation using a nonlinear spectral wave model with nonlinear triad interaction and frequency dependent breaking. Spectral transformation in SWAN may be improved by adopting some of the formulations found in Sheremet et al. (2011). Furthermore comparative testing needs to be conducted to look at other reef geometries and cases with realistic bottom friction. The accuracy of predictions of other metrics (e.g., skewness and asymmetry of velocity and acceleration), not just bulk wave height, that are also important for predicting wave driven currents and sediment transport need to be investigated. In general, the capabilities of these non-reef / steep slope specific beach models shows promise when applied to these environments.

Acknowledgements

This project forms part of a PhD study by M. Buckley at The University of Western Australia and is supported by an International Postgraduate Research Scholarships. R. Lowe was supported by an Australian Research Council Future Fellowship.

References

Apotsos, A., Raubenheimer, B., Elgar, S. and Guza, R.T., 2008. Testing and calibrating parametric wave transformation models on natural beaches. *Coastal Engineering*, 55(3): 224-235.

Apotsos, A., Raubenheimer, B., Elgar, S., Guza, R.T. and Smith, J.A., 2007. Effects of wave rollers and bottom stress on wave setup. *Journal of Geophysical Research*, 112(C2).

Battjes, J.A. and Janssen, J.P.F.M., 1978. Energy loss and set-up due to breaking of random waves. *Proc. 16th Int. Conf. Coastal Engineering, ASCE*: 569-587.

Booij, N., Ris, R.C. and Holthuijsen, L.H., 1999. A third-generation wave model for coastal regions 1. Model description and validation. *Journal of Geophysical Research C: Oceans*, 104(C4): 7649-7666.

Buckley, M.L., Wei, Y., Jaffe, B.E. and Watt, S.G., 2011. Inverse modeling of velocities and inferred cause of overwash that emplaced inland fields of boulders at Anegada, British Virgin Islands. *Natural Hazards*: 1-17.

Cienfuegos, R., Barthélemy, E. and Bonneton, P., 2010. Wave-breaking model for Boussinesq-type equations including roller effects in the mass conservation equation. *Journal of Waterway, Port, Coastal and Ocean Engineering*, 136(1): 10-26.

Demirbilek, Z. and Nwogu, O.G., 2007. Boussinesq Modeling of Wave Propagation and Runup over Fringing Coral Reefs, Model Evaluation Report. *Data Report. ERDC/CHL TR-07-12, Coastal and Hydraulics Laboratory*

Demirbilek, Z., Nwogu, O.G. and Ward, D.L., 2007. Laboratory Study of Wind Effect on Runup over Fringing Reefs, Report 1: Data Report. *ERDC/CHL TR-07-4, Coastal and Hydraulics Laboratory*.

Feddersen, F., Gallagher, E.L., Guza, R.T. and Elgar, S., 2003. The drag coefficient, bottom roughness, and wave-breaking in the nearshore. *Coastal Engineering*, 48(3): 189-195.

Filipot, J.-F. and Cheung, K.F., 2012. Spectral wave modeling in fringing reef environments. *Coastal Engineering*, 67: 67-79.

Gourlay, M.R. and Colleter, G., 2005. Wave-generated flow on coral reefs—an analysis for two-dimensional horizontal reef-tops with steep faces. *Coastal Engineering*, 52(4): 353-387.

Hardy, T.A. and Young, I.R., 1996. Field study of wave attenuation on an offshore coral reef. *J. Geophys. Res.*, 101(C6): 14311-14326.

Hearn, C.J., 1999. Wave-breaking hydrodynamics within coral reef systems and the effect of changing relative sea level. *J. Geophys. Res.*, 104(C12): 30007-30019.

Hoeke, R., Storlazzi, C. and Ridd, P., 2011. Hydrodynamics of a bathymetrically complex fringing coral reef embayment: Wave climate, in situ observations, and wave prediction. *Journal of Geophysical Research-Oceans*, 116.

Lowe, R.J., Falter, J.L., Bandet, M.D., Pawlak, G., Atkinson, M.J., Monismith, S.G. and Koseff, J.R., 2005. Spectral wave dissipation over a barrier reef. *J. Geophys. Res.*, 110(C4): C04001.

Lowe, R.J., Falter, J.L., Monismith, S.G. and Atkinson, M.J., 2009. A numerical study of circulation in a coastal reef-lagoon system. *J. Geophys. Res.*, 114(C6): C06022.

Madsen, P.A., Sørensen, O.R. and Schäffer, H.A., 1997. Surf zone dynamics simulated by a Boussinesq type model. Part I. Model description and cross-shore motion of regular waves. *Coastal Engineering*, 32(4): 255-287.

Mansard, E.P.D. and Funke, E. R., 1980. Measurement of incident and reflected spectra using a least squares method. *17th International Conference on Coastal Engineering, Sydney, Australia*. pp. 95–96

Massel, S.R. and Gourlay, M.R., 2000. On the modelling of wave breaking and set-up on coral reefs. *Coastal Engineering*, 39(1): 1-27.

Nelson, R.C., 1987. Design wave heights on very mild slopes: an experimental study. *Civil Engineering Transactions*, 29: 157–161.

Péquignet, A.C.N., Becker, J.M., Merrifield, M.A. and Aucan, J., 2009. Forcing of resonant modes on a fringing reef during tropical storm Man-Yi. *Geophysical Research Letters*, 36(3).

Pomeroy, A., Lowe, R., Symonds, G., Van Dongeren, A. and Moore, C., 2012. The dynamics of infragravity wave transformation over a fringing reef. *Journal of Geophysical Research-Oceans*, 117.

Reniers, A.J.H.M.B., J.A., 1997. A laboratory study of longshore currents over barred and non-barred beaches. *Coastal Engineering*, 30(1-2): 1-21.

Roelvink, D., Reniers, A., van Dongeren, A., van Thiel de Vries, J., McCall, R. and Lescinski, J., 2009. Modelling storm impacts on beaches, dunes and barrier islands. *Coastal Engineering*, 56(11-12): 1133-1152.

Roelvink, J.A., 1993. Dissipation in random wave groups incident on a beach. *Coastal Engineering*, 19(1–2): 127-150.

Schäffer, H.A., Madsen, P.A. and Deigaard, R., 1993. A Boussinesq model for waves breaking in shallow water. *Coastal Engineering*, 20(3–4): 185-202.

Sheremet, A., Kaihatu, J.M., Su, S.F., Smith, E.R. and Smith, J.M., 2011. Modeling of nonlinear wave propagation over fringing reefs. *Coastal Engineering*, 58(12): 1125-1137.

Smit, P., Zijlema, M. and Stelling, G., 2013. Depth-induced wave breaking in a non-hydrostatic, near-shore wave model. *Coastal Engineering*, 76: 1-16.

Storlazzi, C.D., Elias, E., Field, M.E. and Presto, M.K., 2011. Numerical modeling of the impact of sea-level rise on fringing coral reef hydrodynamics and sediment transport. *Coral Reefs*, 30: 83-96.

Svendsen, I.A., 1984. Mass flux and undertow in a surf zone. *Coastal Engineering*, 8(4): 347-365.

Symonds, G., Black, K.P. and Young, I.R., 1995. Wave-driven flow over shallow reefs. *J. Geophys. Res.*, 100(C2): 2639-2648.

Torres-Freyermuth, A., Marino-Tapia, I., Coronado, C., Salles, P., Medellin, G., Pedrozo-Acuna, A., Silva, R., Candela, J. and Iglesias-Prieto, R., 2012. Wave-induced extreme water levels in the Puerto Morelos fringing reef lagoon. *Natural Hazards and Earth System Sciences*, 12(12): 3765-3773.

Van Dongeren, A., Lowe, R., Pomeroy, A., Trang, D.M., Roelvink, D., Symonds, G. and Ranasinghe, R., 2013. Numerical modeling of low-frequency wave dynamics over a fringing coral reef. *Coastal Engineering*, 73: 178-190.

Zijlema, M., 2012. Modeling Wave Transformation Across a Fringing Reef using SWASH. *Coastal Engineering Proceedings*, 1(33)(currents.26).

Zijlema, M., Stelling, G. and Smit, P., 2011. SWASH: An operational public domain code for simulating wave fields and rapidly varied flows in coastal waters. *Coastal Engineering*, 58(10): 992-1012.

Zijlema, M. and Stelling, G.S., 2008. Efficient computation of surf zone waves using the nonlinear shallow water equations with non-hydrostatic pressure. *Coastal Engineering*, 55(10): 780-790.

Zijlema, M., van Vledder, G.P. and Holthuijsen, L.H., 2012. Bottom friction and wind drag for wave models. *Coastal Engineering*, 65: 19-26.